RSC Advances

ROYAL SOCIETY OF CHEMISTRY

www.rsc.org/advances

Realization of flexible and mechanically robust Ag mesh transparent electrode and its application in PDLC device

Liangfei Qi[1,2], Jia Li[*1], Chaoting Zhu[1], Ye Yang[1], Shijin Zhao[2], Weijie Song[*1]

1. Ningbo Institute of Material Technology and Engineering, Chinese Academy of Sciences, Ningbo, 315201, P. R. China

2. Institute of Materials Science, Shanghai University, Shanghai, 200072, P. R. China

Tel & Fax: 86-574-87913375, Email: lijia@nimte.ac.cn

Abstract: In this paper, flexible Ag electrodes with a hexagonal micromesh structure were fabricated on PET substrate using photolithography technique. The effect of film thickness on optical and electrical properties of Ag electrodes was investigated systematically. Furthermore, these flexible transparent Ag mesh electrodes were firstly applied to the Polymer dispersed liquid crystal (PDLC) device and its performance was evaluated. All the Ag electrodes exhibited a high average transmittance of about 80.2-85.0% in the visible range (400-800 nm), and the minimum sheet resistance value reached 8.2 Ω/sq. The prepared Ag mesh also showed an excellent performance of adhesion and bending, demonstrating their superior durability. The PDLC device based on Ag mesh electrode showed comparable performance with that using ITO electrode, indicating that Ag mesh film can be a good substitution for ITO electrode in PDLC device and may find practical application in large area flexible device.

Keywords: transparent conductive electrodes, Ag mesh, flexible, durable, PDLC

1 Introduction

Recent years, flexible devices have become an emerging tendency and are finding various applications in daily life.[1] Polymer dispersed liquid crystal (PDLC), which has a basis structure of liquid crystals sandwiched by a pair of electrodes on flexible PET substrate, is a promising device to modulate electro-optic performance in display devices and smart windows.[2] Most commonly, the transparent conducting electrodes (TCEs) used for flexible device nowadays are still based on transparent conductive oxide, particularly Indium-tin oxide (ITO) due to its excellent optical transmittance and low sheet resistance in visible range of the electromagnetic spectrum.[3] However, ITO electrode has drawback such as high price due to In metal deficiency and brittleness due to its ceramic nature, which restrain its application in large-scale flexible devices.[4] In recent decades, alternative TCEs have being investigated to replace ITO, including carbon nanotube networks,[5,6] graphene,[7] conductive polymers,[8,9] random nanowires[10,11] and Ag mesh.[12-14] Among these, Ag mesh electrode is a promising candidate because it offers good optical transparency and high electrical conductivity as well as superior mechanical stability.[15] It has been demonstrated theoretically and experimentally that their optical and electrical properties could be tuned relatively independently by changing the relevant geometrical parameters of Ag mesh structures such as line width (w), period (p), and thickness (h).[12, 16, 17]

Generally, the network structure of Ag mesh electrode can be designed to be random or regular shape. Random Ag mesh electrodes were fabricated by some novel method such as nanosphere lithography,[18] electrospun nanotroughs,[19] inject printing, [20, 21] laser sintering,[22] and methods based on coffee ring effect.[23,24] Recently, random Au meshes fabricated by grain lithography have demonstrated 83% transmittance at 20 Ω/sq.[25] Ag networks on PET are prepared by depositing Ag film inside the gaps of a cracked TiO_2 gel mold, which has a high transmittance of 88% at 10 Ω/sq.[26] Ag gratings of 78% transmittance at 23 Ω/sq have been investigated using nanoimprint lithography.[27] However, these methods could give rise to problems of complex treatments and nonuniform performances which rely on the repeatability of molding.

On the other hand, physical lithography method such as electron beam lithography, Nanoimprint and photolithography have been used to prepare uniform and ordered Ag meshes, which is in favor of the repeatability and device stability thanks to its uniform structure. However, the two previous methods are relatively costly and not scalable. As a conventional technique, photolithography has been applied for large-area patterning.[28] Ag mesh electrodes fabricated by photolithography method show a transmittance of 74% at about 7 Ω/sq.[29,30] While, these electrodes are mostly prepared on rigid substrates, few works are about flexible substrates. Furthermore, to our knowledge, the fabrication of PDLC device with Ag mesh film acting as electrodes has not been reported.

In this work, we demonstrated a hexagonal Ag mesh on PET substrates directly by photolithography, which act as the electrode for PDLC device. the effects of film

thickness on their performance were investigated systematically. The optical, electrical and mechanical properties of this Ag mesh film as well as the performance of the PDLC device are evaluated in detail.

2 Experimental

2.1 Fabrication procedures

Polyethylene terephthalate (PET) substrates were sequentially cleaned in ethanol, acetone and deionized water by ultrasonication each for 2 minutes, followed by drying with nitrogen gas. Photolithography was performed in a yellow room inside a cleanroom. Fig. 1 shows the schematic diagram of the fabrication of Ag mesh film. A KMP e3130b photoresist (Kempur Microelectronics, China) was first spin coated on the PET substrates at 3500 rpm for 35 seconds and prebaked at 90℃ for 90 seconds. After exposed to 365 nm UV light using ABM/6/350/NUV/DCCD/M Manual Mask Aligner System (ABM, USA) for 40 seconds, the photoresist was developed in KMP PD238 developer (Kempur Microelectronics, China) for 40 seconds. Ag films of different thickness (10 nm, 25 nm, 40 nm, 55 nm, 70 nm) were sputtered onto the samples after a 5 nm thick Cr deposition acting as an adhesive layer using JCP-350M2 magnetron sputtering apparatus (Technol, China). Finally, Ag mesh films were patterned after a lift-off process in acetone. The line width and periodicity were set as 4 μm and 100 μm, respectively.

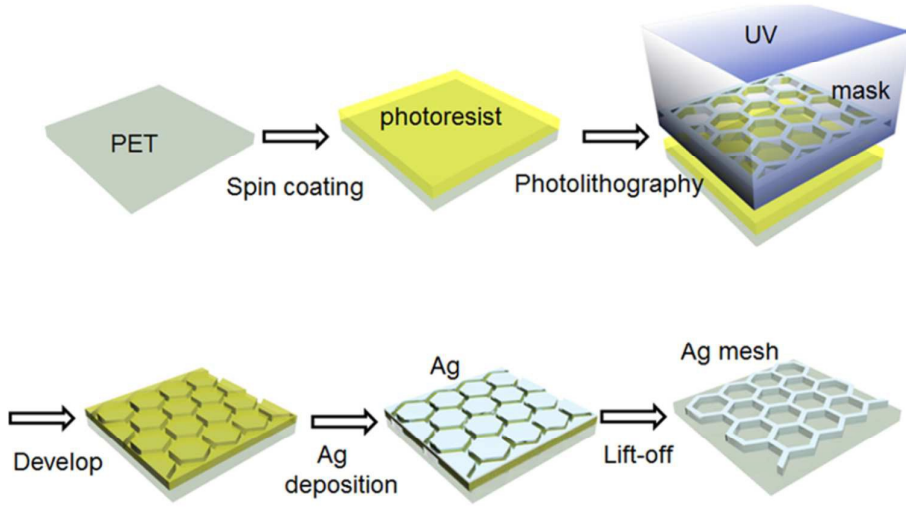

Fig.1 Schematic of the Ag mesh film fabrication process.

PDLC device was fabricated using above prepared Ag mesh as transparent electrode. NOA 65(Norland products) and nematic LC E7(Yantai Xianhua Chem-Tech. Co., Ltd) were used as the pre-polymer and nematic LC mixture, respectively. The mixing ratio of NOA 65 and E7 was fixed at 2:3. Silica microsphere with a mean diameter of 60 μm was used as spacers to control the thickness of PDLC device. The substrates, Ag mesh coated PET films were cut into 40 mm×40 mm pieces. Before using as electrode, a thin layer of ZnO:Al with the thickness of 50 nm was deposited on Ag mesh for protection and ensuring the uniform conductivity of the electrode. The LC/NOA65 mixture was coated and spread on the bottom Ag mesh electrode and then covered by a top Ag mesh electrode. The sandwich structure was then exposed to UV light with the intensity of 15 mW/cm^2 for 8 min.

2.2 characterization and measurement

The surface morphologies of Ag mesh film was examined by field emission scanning electron microscope (FE-SEM, Hitachi S-4800). The optical transmittance

and haze of the Ag mesh films were obtained at room temperature using a UV-Vis-NIR spectrophotometer (Agilent, Cary 5000). The sheet resistance was measured by a four-point probe system (ST-2258A). The thicknesses of the films were calculated and conformed using atomic force microscopy (Veeco, Dimension3100V). To investigate the mechanical properties, a bending test was carried out with a home-made equipment. The adhesion test was performed using a 12.7 mm wide 3M scotch tape to attach onto the Ag mesh film and then peeled off from the sample. To evaluate the performance of the fabricated PDLC device, the specular transmittance-voltage curve was measured using spectroscopic ellipsometer (model M2000DI) with an alternating voltage potential (0-120 V) applying across the device.

3 Results and discussion

3.1 microstructure of Ag mesh films

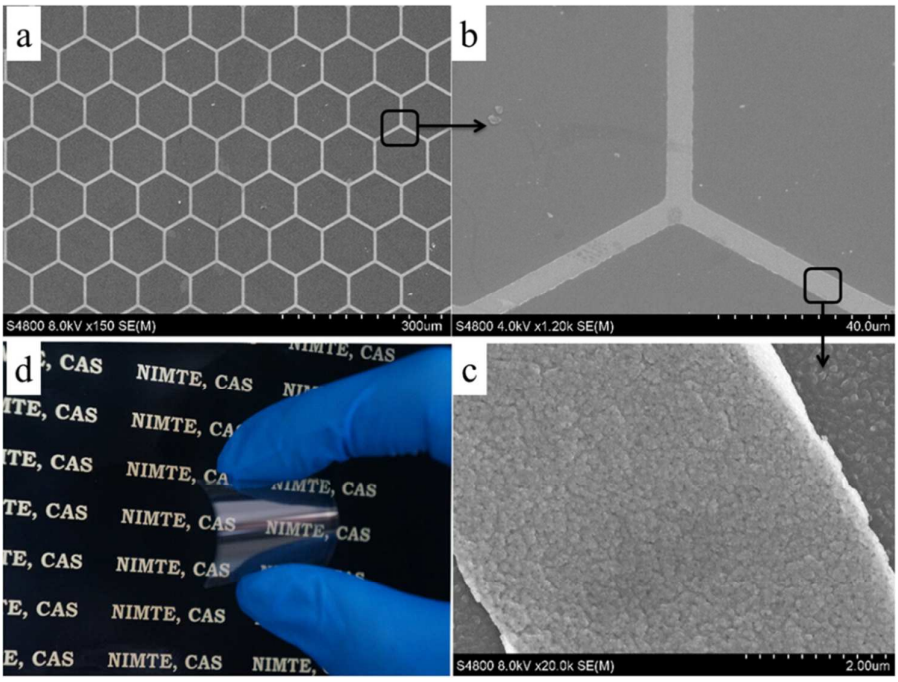

Figure 2 (a) SEM image of fabricated Ag mesh on PET substrate; (b) (c) enlarged SEM images of Ag films; (d) optical image of Ag mesh film on PET.

Five hexagonal Ag mesh films with the thickness of 10, 25, 40, 55 and 70 nm were prepared on PET substrates. Fig. 2 shows the SEM images and the optical image of the fabricated 70 nm Ag micromesh patterns on PET substrate. Fig. 2a indicates an uniform and perfect metal network, and the enlarged image (Fig. 2b) shows that the Ag wires are well connected with straight boundary and smooth surface. The Ag film deposited by magnetic sputtering on amorphous PET substrate indicated good quality with compact and homogenous distribution of small particles of about 200 nm (Fig. 2c). The line width measured from Fig. 2c is about 5.5 μm, deviating from the designed value of 4 μm for the mask, which may because of the deviation of the mask fabrication and photolithography process. The uniform and compact Ag film morphologies benefit its conductivity and mechanical performances. Fig. 2d shows the optical image of Ag mesh film on PET substrate, the letters on paper can clearly be seen through the Ag mesh transparent film.

3.2 optical and electrical properties of Ag mesh films

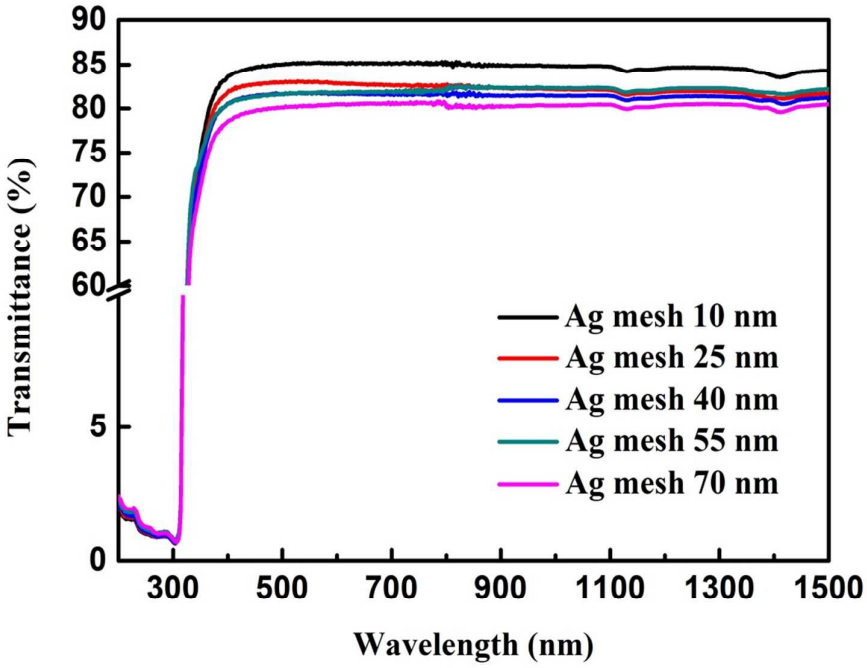

Figure 3 Transmittance of Ag mesh on PET substrate with 10, 25, 40, 55, and 70 nm thickness.

Figure 3 shows the optical transmittance spectra of fabricated Ag mesh with different thickness, all transmittance spectral measurements were referenced to air. Ag mesh films have almost constant transmittance values in the whole wavelength range. The average transmittance of the Ag mesh films on PET with 10, 25, 40, 55, and 70 nm film thickness in the entire visible wavelength range (400-800 nm) were 85.0%, 82.7%, 81.5%, 81.6% and 80.2%, respectively. Which indicates all the Ag mesh films possess an uniform and high transmittance >80% in a broad wavelength range. It is noticed that there is a slight decline while the film thickness increasing to 70 nm, may because of the lager line width. Taken the open area ratio of the Ag mesh as 92% and the transmittance of PET substrate as 90%,[31] the theoretically transmittance of Ag mesh film should be around 82.8%. The transmittance of Ag mesh of 10 nm film

thickness in our experiment is 85%, which is attributed to the transparency of Ag film when the thickness is less than 10 nm.[32]

Sheet resistance values were measured and summarized in Table 1. The measured sheet resistance of Ag mesh film with thickness of 10, 25, 40, 55 and 70 nm were 108.3, 42.5, 18.1, 12.3, and 8.2 Ω/sq, respectively, which demonstrated a significant reduction when the film thickness increased from 10 nm to 70 nm. It indicated that the sheet resistance of the transparent metal electrode could be controlled relatively independently by adjusting the thickness of the Ag mesh without sacrificing the optical transmittance, which is far different from the other types of TCEs including TCOs, CNTs, and nanowires, where there is a trade-off between optical transmittance and sheet resistance, making it a great challenge for these TCEs to obtain good optical and electrical properties simultaneously.

Table 1. Optical and electrical parameters of transmittance, sheet resistance, figure of merit and haze for Ag mesh films and ITO film.

	Thickness (nm)	T (%)	R (Ω/sq)	FOM	Haze (%)
Ag mesh film	10	85.0	108.3	20.5	1.1
	25	82.7	42.5	44.5	1.7
	40	81.5	18.1	96.7	2.2
	55	81.6	12.3	143.2	2.6
	70	80.2	8.2	194.7	2.2
ITO film [30]	—	85.7	13.4	175.5	—

To evaluate the effect of mesh thickness on the overall performance of the TCEs, Figure of Merit (FOM) was determined, which was the ratio of the electrical conductance and the optical conductance. The equation of DC/OPT is as follows:

$$T = \left(1 + \frac{188.5}{R}\frac{\sigma_{opt}}{\sigma_{dc}}\right)^{-2} \quad (1)$$

where R and T are the measured sheet resistance and transmittance at 550 nm,

respectively. The data of ITO film from reference 30 are also listed for comparison. The FOM values for five Ag mesh films of 10, 25, 40, 55 and 70 nm are 20.5, 44.5, 96.7, 143.2 and 194.7, respectively. A significant improvement was suggested with the increasing film thickness, which resulted from the enhancement of electrical conductivity over-compensated for the reduction in optical transparency. High FOM is preferred for TCE applications, the maximum FOM of our Ag mesh of 70 nm is 194.7, which is better than some of the best values for TCEs of PEDOT:PSS (36),[33] graphene (120),[7] metal nanowires (65-160),[8] and comparable to ITO film (175.5) and metal meshes (171).[29]

Haze value of different Ag mesh films are also measured and shown in Table 1. The haze value is defined as the ratio of diffusive transmittance to total transmittance, with an illumination from the glass side. The thicker the Ag thickness, the higher the haze value. The haze value reached saturated after the Ag thickness larger than 40 nm. Although the value was far less than that of Ag nanowires reported in literature, a low haze value not larger than 1% is important to its application, especially for touch screen application.

3.3 mechanical properties of Ag mesh films

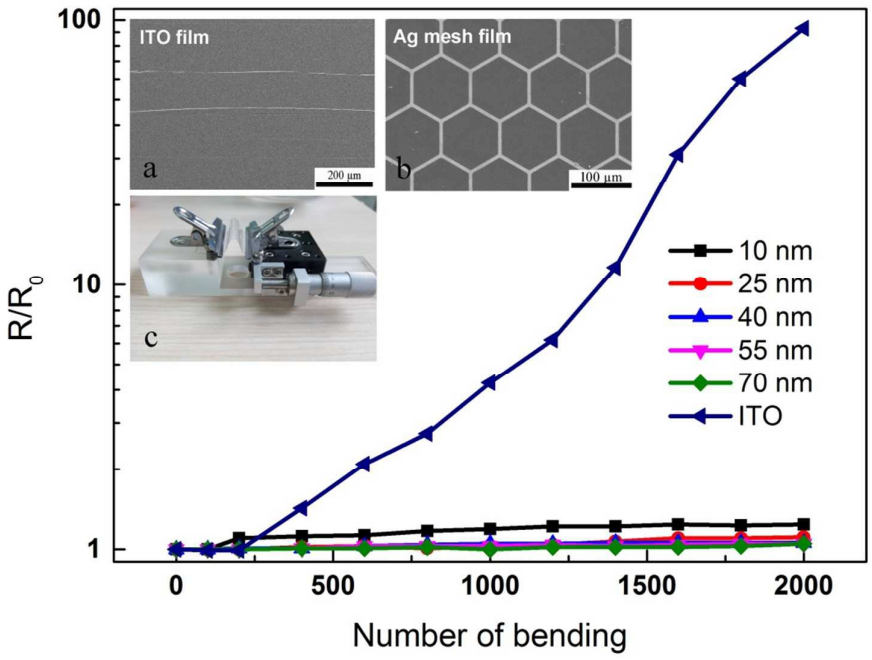

Figure 4 Effect of repeated bending on the sheet resistance of ITO and Ag mesh. SEM images of ITO (a) and Ag mesh (b) after 2000 cyclic bending; (c) test setup of cyclic bending.

Besides electrical and optical properties, mechanical stability of the TCE film on flexible substrate is also vital for its applications. To further evaluate the mechanical stability of the Ag mesh transparent electrodes, cyclic bending test and adhesive tape test are performed. Fig. 4 shows the bending test, the original length of Ag mesh on PET is L=30 mm, the deformation of each cycle is dL=15 mm, therefore, the bending radius is R=6.7 mm, and strain is ε =1.0% according to $\varepsilon = h/2R$ (where h is the whole thickness of Ag mesh and PET, R is the bending radius[34]). Same measurement was operated on ITO coated PET as a comparison. As can be seen in Fig. 4, commercial ITO's resistance increased significantly and reached to 1200.0 Ω after 2000 bending cycles. Fig. 4a shows the SEM image of ITO film after 2000 bending

cycles. Some micro cracks were developed perpendicular to the bending direction, which was due to the brittleness of ITO film. The formation of these micro cracks lead to a deteriorative electrical conductivity during repeated deformation. On the contrast, the changes in resistance for Ag mesh films were far less than that of ITO film. The mechanical performance of Ag mesh films were influenced by the film thickness. The 10 nm Ag mesh film showed an inferior performance after bending, which may be due to the small film thickness. Increasing the film thickness demonstrated an apparent improvement of stability (showed in Fig. S2). For the samples with the Ag thickness of 70 nm, the change in resistance was less than 5% of its original value (from 10.0 to 10.2 Ω) throughout 2000 bending cycles. The SEM image of Ag mesh after 2000 bending cycles (Fig. 4b) also confirmed that Ag mesh structure remained unchanged with no cracks could be observed.

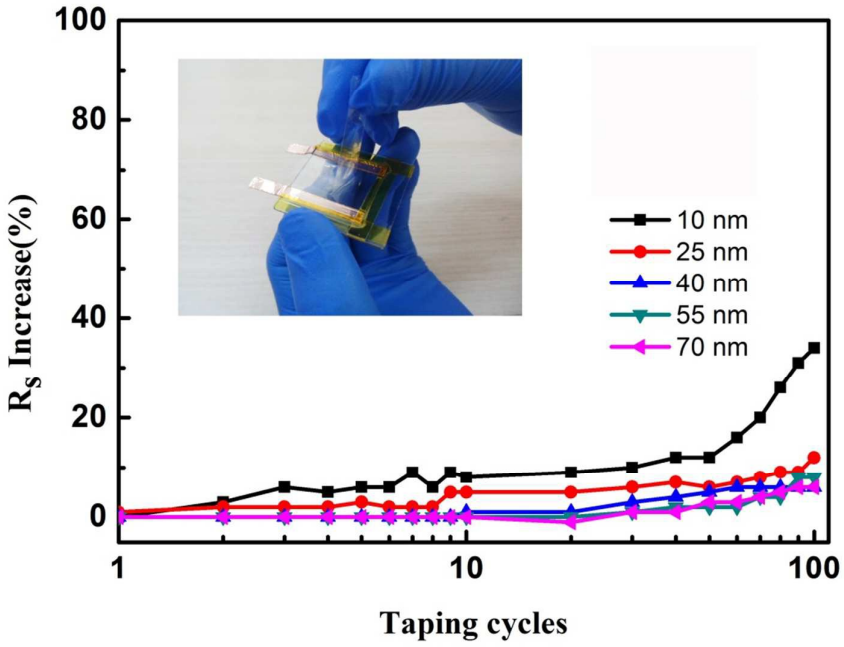

Figure 5 Changes in the sheet resistance of the Ag mesh films during the adhesive tape test.

Tape test is also conducted to evaluate the adhesion between Ag mesh film and PET substrate. Fig. 5 shows the changes in sheet resistance of Ag mesh films with different thickness during the repeated adhesive tape test. The adhesive properties improved with the increase of Ag mesh film thickness. The inferior performance of 10 nm sample was due to the peeling off the mesh film from the substrate in some part because of low thickness (as shown in Fig. S3). The changes of the resistance value decreased and kept steady for thicker films. For the sample with 70 nm Ag film, the sheet resistance changed slightly ($<$5%) after 100 cycles, which is superior to Ag nanowires films.[35] Both of the bending test and tape test all indicated that our Ag mesh electrodes demonstrate excellent flexibility and adhesion, as well as high optical and electrical properties, which may benefit their applications in optoelectronic devices.

3.4 performance of PDLC device with Ag mesh electrodes

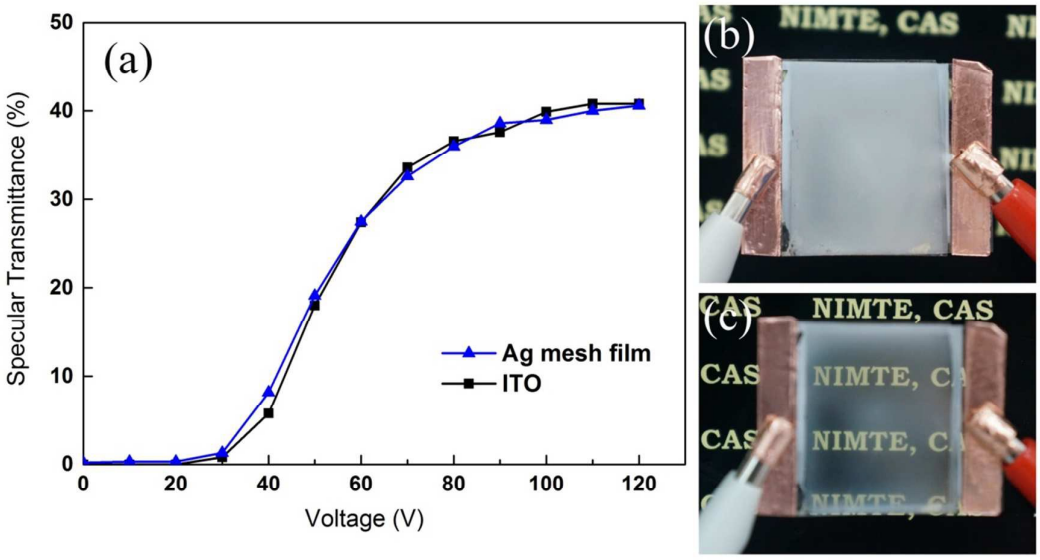

Figure 6 (a) the specular transmittance-voltage curve of the PDLC device with Ag mesh and ITO electrode. Photographic images of PDLC device with Ag mesh electrode at (b) off state and (c) on state.

PDLC device was fabricated to evaluate its performance with Ag mesh film as electrode. The Ag mesh film with 70 nm Ag thickness was chosen for device fabrication. A device using commercial PET/ITO film with almost the same sheet resistance value (8 Ω/sq, brought from KDX Co., Ltd.) was prepared at the same conditions for comparison. Conductive copper tape was stuck on each electrode for better contact. Fig. 6(a) shows the specular transmittance-voltage curve of the PDLC devices at the wavelength of 550 nm using Ag mesh film and ITO film as electrodes, respectively. The device with Ag mesh film as electrode shows almost the same performance as that with ITO electrode. The specular transmittance value is around zero when the voltage is below 20 V, indicating an off state of the device. A linear increase of transmittance with steep slope between 30 V and 70 V can be observed.

After that, the specular transmittance tend towards saturation with increasing voltage above 70 V. The maximum specular transmittance is 41%. In general, the driving voltage can be defined at the applied voltage of an optical transmittance of 90% of the maximum value,[36] thus the driving voltage in this device is around 80 V. Since the thickness of the cell gap of this device is 60 μm, which leading to higher driving voltage and lower specular transmittance comparing with those devices with thinner cell gap.[37] Fig. 6 (b) and (c) shows the photographic images of the device with Ag mesh electrode at off and on states, respectively. An AC voltage of 100 V was selected as the on state voltage. At the off state, the device presents opaque color with good scattering properties. After applying voltage, the device became transparent with some milky color indicating a relatively high haze value. The PDLC device with Ag mesh electrode shows high contrast ratio and uniformity in both on and off states. It indicates that Ag mesh film can be a good substitution for ITO electrode in PDLC device and may find application in large area flexible device fabrication.

4 Conclusions

We have demonstrated a hexagonal Ag mesh transparent conductive electrode on PET flexible substrate. The Ag mesh is patterned by photolithograpy with a fixed line width of 4 μm and periodicity 100 μm. Five different Ag mesh films were prepared with thickness from 10 nm to 70 nm. All the samples showed high optical transmittance >80% as well as good conductivity of 8 Ω/sq at a film thickness of 70 nm. This can be used to change the optical transmittance and electrical resistance independently by adjusting the film thickness, line width and periodicity. The Ag

mesh produced by photolithograpy and magnetic sputtering on flexible substrate also showed an excellent stability in terms of adhesion and bending. Furthermore, this Ag mesh electrode can be a good electrode candidate for PDLC device with high contrast ratio and uniformity at both on and off states.

Acknowledgement

This work was supported by the Natural Science Foundation of China (No. 21377063), Zhejiang Natural Science Foundation (No. LY15F040004) and the program for Ningbo Key Laboratory of Silicon and Organic Thin Film Optoelectronic Technologies.

References

(1) J. Z. Song, H. B. Zeng, *Angew. Chem. In. Ed.*, 2015, 54, 9760-9774.

(2) Y. Kim. D. Jung, S. Jeong, K. Kim, W. Choi, Y. Seo, *Curr. Appl. Phys.*, 2015, 15, 292-297

(3) M. Layani, A. Kamyshny and S. Magdassi, *Nanoscale*, 2014, 6, 5581-5591.

(4) K. S. Kim, Y. Zhao, H. Jang, S. Y. Lee, J. M. Kim, K. S. Kim, J.-H. Ahn, P. Kim, J.-Y. Choi and B. H. Hong, *Nature*, 2009, 457, 706-710.

(5) Z. C. Wu, Z. H. Chen, X. Du, J. M. Logan, J. Sippel, M. Nikolou, K. Kamaras, J. R. Reynolds, D. B. Tanner, A. F. Hebard and A. G. Rinzler, *Science*, 2004, 305, 1273-1276.

(6) D. S. Hecht, A. M. Heintz, R. Lee, L. Hu, B. Moore, C. Cucksey and S. Risser,

Nanotechnology, 2011, 22, 075201.

(7) J. H. Zhu, M. J. Chen, Q. L. He, L. Shao, S. Y. Wei, Z. H. Guo. *Rsc. Adv.*, 2013, 3, 22790-22824.

(8) S.-I. Na, S.-S. Kim, J. Jo and D.-Y. Kim, *Adv. Mater.*, 2008, 20, 4061-4067.

(9) K. Ellmer, *Nat. Photonics*, 2012, 6, 808-816.

(10) Q. J. Huang, W. F. Shen, W. J. Song, *RSC Adv.*, 2015, 5, 45836-45842.

(11) J. Z. Song, J. H. Li, J. Y. Xu, H. B. Zeng, *Nano Lett.*, 2014, 14, 6298-6305.

(12) J. van de Groep, P. Spinelli and A. Polman, *Nano Lett.*, 2012, 12, 3138-3144.

(13) N. Kwon, K. Kim, S. Sung, I. Yi and I. Chung, *Nanotechnology*, 2013, 24, 235205.

(14) M.-G. Kang, H. J. Park, S. H. Ahn and L. J. Guo, *Sol. Energy Mater. Sol. Cells.*, 2010, 94, 1179-1184.

(15) H.-J. Kim, S.-H. Lee, J. Lee, E.-S. Lee, J.-H. Choi, J.-H. Jung, J.-Y. Jung and D.-G. Choi, *Small*, 2014, 10, 3767-3774.

(16) P. B. Catrysse and S. Fan, *Nano Lett.*, 2010, 10, 2944-2949.

(17) F. Afshinmanesh, A. G. Curto, K. M. Milaninia, N. F. van Hulst and M. L. Brongersma, *Nano Lett.*, 2014, 14, 5068-5074.

(18) T. C. Gao, B. M. Wang, B. Ding, J. K. Lee and P. W. Leu, *Nano Lett.*, 2014, 14, 2105-2110.

(19) H. Wu, D. Kong, Z. Ruan, P.-C. Hsu, S. Wang, Z. Yu, T. J. Carney, L. Hu, S. Fan and Y. Cui, *Nat. Nanotechnol.*, 2013, 8, 421-425.

(20) B. Y. Ahn, D. J. Lorang and J. A. Lewis, *Nanoscale*, 2011, 3, 2700-2702.

(21) Y. Li, L. Mao, Y. Gao, P. Zhang, C. Li, C. Ma, Y. Tu, Z. Cui and L. Chen, *Sol. Energy Mater. Sol. Cells*, 2013, 113, 85-89.

(22) S. Hong, J. Yeo, G. Kim, D. Kim, H. Lee, J. Kwon, H. Lee, P. Lee and S. H. Ko, *ACS Nano*, 2013, 7, 5024-5031.

(23) M. Layani, M. Gruchko, O. Milo, I. Balberg, D. Azulay and S. Magdassi, *ACS Nano*, 2009, 3, 3537-3542.

(25) Z. Zhang, X. Zhang, Z. Xin, M. Deng, Y. Wen and Y. Song, *Adv. Mater.*, 2013, 25, 6714-6718.

(25) C. F. Guo, T. Sun, Q. Liu, Z. Suo and Z. Ren, *Nat. Commun.*, 2014, 5, 3121.

(26) B. Han, K. Pei, Y. Huang, X. Zhang, Q. Rong, Q. Lin, Y. Guo, T. Sun, C. Guo, D. Carnahan, M. Giersig, Y. Wang, J. Gao, Z. Ren and K. Kempa, *Adv. Mater.*, 2014, 26, 873-877.

(27) M.-G. Kang, M.-S. Kim, J. Kim and L. J. Guo, *Adv. Mater.*, 2008, 20, 4408-4413.

(28) S. M. Huang, L. M. Dai, A. W. H. Mau, *Adv. Mater.*, 2002, 14, 1140-1143.

(29) F. L. M. Sam, C. A. Mills, L. J. Rozanski and S. R. P. Silva, *Laser Photonics Rev.*, 2014, 8, 172-179.

(30) J. W. Lim, Y. T. Lee, R. Pandey, T. H. Yoo, B. I. Sang, B. K. Ju, K. Hwang do and W. K. Choi, *Opt. Express*, 2014, 22, 26891-26899.

(31) K. Neyts, A. Real, M. Marescaux, S. Mladenovski and J. Beeckman, *J. Appl. Phys.*, 2008, 103, 093113.

(32) H. Kang, S. Jung, S. Jeong, G. Kim and K. Lee, *Nat. commun.*, 2015, 6.

(33) Y. H. Kim, C. Sachse, M. L. Machala, C. May, L. Muller-Meskamp and K. Leo,

Adv. Funct. Mater., 2011, 21, 1076-1081.

(34) J. L. Ni, X. F. Zhu, Z. L. Pei, J. Gong, C. Sun and G. P. Zhang, *J. Phys. D: Appl. Phys.*, 2009, 42, 175404.

(35) Q. Huang, W. Shen, X. Fang, G. Chen, Y. Yang, J. Huang, R. Tan and W. Song, *ACS Appl. Mater. Interfaces*, 2015, 7, 4299-4305.

(36) J. Kim and J. I. Han, *Electronic Mater. Lett.*, 2014, 10, 665-669.

(37) H. H. Khaligh, K. Liew, Y. Han, N. M. Abukhdeir and I. A. Goldthorpe, *Sol. Energy Mater. Sol.Cells*, 2015, 132, 337-341.

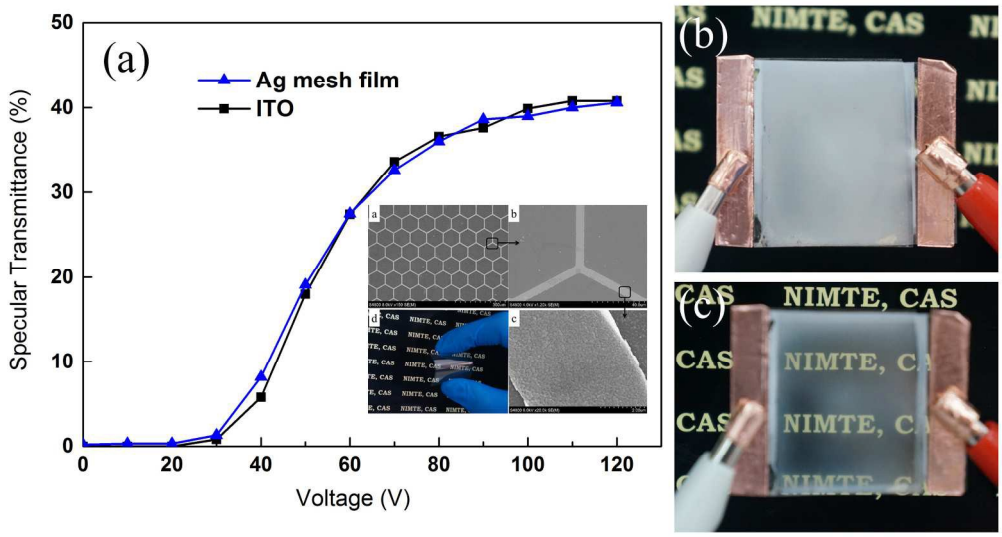

196x109mm (300 x 300 DPI)